Thin Ising films with competing walls: A Monte Carlo study

K. Binder

Institut für Physik, Johannes Gutenberg-Universität Mainz, Staudinger Weg 7, D-55099 Mainz, Germany

D. P. Landau

Center for Simulational Physics, The University of Georgia, Athens, Georgia 30602

A. M. Ferrenberg

Center for Simulational Physics and University Computing and Networking Services, The University of Georgia, Athens, Georgia 30602

Ising magnets with a nearest neighbor ferromagnetic exchange interaction J on a simple cubic lattice are studied in a thin film geometry using extensive Monte Carlo simulations. The system has two large $L \times L$ parallel free surfaces, a distance D apart from each other, at which competing surface fields act, i.e., $H_D = -H_1$. In this geometry, the phase transition occurring in the bulk at a temperature T_{cb} is suppressed, and instead one observes the gradual formation of an interface between coexisting phases stabilized by the surface fields. While this interface is located in the center of the film for temperatures $T_c(D) < T \lesssim T_{cb}$, and the average order parameter of the film is hence zero, at $T_c(D)$ we observe the interface localization-delocalization transition predicted by Parry and Evans [Phys. Rev. Lett. **64**, 439 (1990); Physica A **181**, 250 (1992)]. For $T < T_c(D)$, there is thus a symmetry breaking, and the interface is located either close to the left wall where $H_1 < 0$ (and the total film magnetization is then positive) or close to the right wall where $H_D = -H_1 > 0$ (and the total magnetization is negative). As predicted, for large D this transition temperature $T_c(D)$ is close to the wetting transition $T_w(H_1)$ of the semi-infinite system, but the transition nevertheless has a two-dimensional Ising character. Due to crossover problems (for $D \to \infty$ the width of the asymptotic Ising region shrinks to zero, and one presumably observes critical wetting in this model) this Ising nature is clearly seen only for rather thin films. For $T_c(D) < T < T_{cb}$ evidence for a correlation length $\xi_{\parallel}$ that varies exponentially with film thickness is obtained and compared to corresponding theoretical predictions.

PACS number(s): 64.60.Fr, 68.45.Gd, 68.35.Rh

I. INTRODUCTION

There has been extensive research on thin films because of their growing technological importance for various applications as well as for their fundamental scientific interest. Here, we focus on the statistical mechanics of phase transitions in a thin film geometry, studying the interplay between confinement (i.e., a "finite size effect") and competing wall forces (i.e., a "surface effect"). It is physically very natural that the two surfaces of a thin film be inequivalent, but theoretically this situation has only occasionally found attention [1–10].

For magnetic systems, of course, it is most natural to consider films whose surfaces do not favor any sign of the order parameter, i.e., where surface magnetic fields are zero, and this case has hence long been considered (see, e.g., [11–13]). However, when we reinterpret an Ising magnet as a lattice gas model for a fluid or as a model for an A,B binary alloy (spins $S_i = \pm 1$ at lattice site i corresponding to the site being occupied or empty, or containing an A atom or B atom, respectively), the situation is completely different: binding energies to the wall translate into surface magnetic fields for the corresponding Ising model [12]. Even if such binding energies are absent (considering, e.g., a "free" surface against vacuum) the effect of "missing neighbors" also contributes to

such a surface field in the Ising spin representation (for explicit demonstrations, see, e.g., Refs. [3,14]). Thus, surfaces are expected to have pronounced effects on the respective phase transitions (condensation in a fluid, unmixing of binary mixtures, etc.), and similar modifications should also occur in thin films of more complex materials such as liquid crystals, microemulsions, polymer blends, and block copolymer mesophases, etc.

In a semi-infinite fluid (or the simple model case of a semi-infinite Ising magnet with a surface field) one can have wetting transitions where the system adapts a state where the surface is coated with an infinitely thick layer of the phase it prefers, separated by an interface from the bulk phase [15–19]. Obviously, in a thin film geometry the walls can be coated only by layers of finite thickness: thus it is really no surprise that in thin films confined between two symmetric walls, both second order and first order wetting transitions are rounded off [20,21]. Only the prewetting transition may still exist [22], for which the surface layer thickness simply jumps discontinuously to a larger value [15,16]. The surface fields then have the effect of shifting the transition between the coexisting phases, which correspond to the coexisting phases in the bulk, away from the bulk location (i.e., of pressure in the fluid, or chemical potential in the mixture, respectively.

Thus, for a fluid that tends to wet the walls, the pressure P at which condensation occurs in a thin film is reduced relative to its bulk coexistence value P_{coex}: "capillary condensation" [14,20–23]. In the magnetic terminology of the Ising model, capillary condensation means a change of sign of the total magnetization, and this first-order transition no longer occurs at zero bulk field (as it would in an infinite system) but at a bulk field inversely proportional to the film thickness, such that it can effectively "cancel" the effect of the surface fields [14,20].

Parry and Evans [5] (and, independently, Albano *et al.* [3], who considered the analogous case of a two-dimensional (2D) Ising system with one-dimensional surfaces) drew attention to Ising models with competing walls: In magnetic terminology, one surface exhibits a positive surface field, the other surface a negative one (in the lattice gas terminology, one wall favors liquid while

the other wall favors the gas). These competing surface effects lead to a rather unusual behavior which we describe, anticipating some simulation results [24,25], in Fig. 1. Here, the profiles of the layer magnetization m_n [which, in lattice gas language, is related to the layer density $\rho_n = (1 - m_n)/2$], the layer internal energy U_n, and the layer susceptibility $\chi_{nn} = \partial M_n / \partial H_n$ are shown for a variety of temperatures. One sees that even for temperatures T exceeding the bulk transition temperature T_{cb} there is already a precursor of an interface, since the surface fields induce a local magnetization near the walls (a negative one at the left wall and a positive one at the right wall). But we expect that this surface-induced order decays exponentially fast with the distance from the walls as one moves towards the interior of the film,

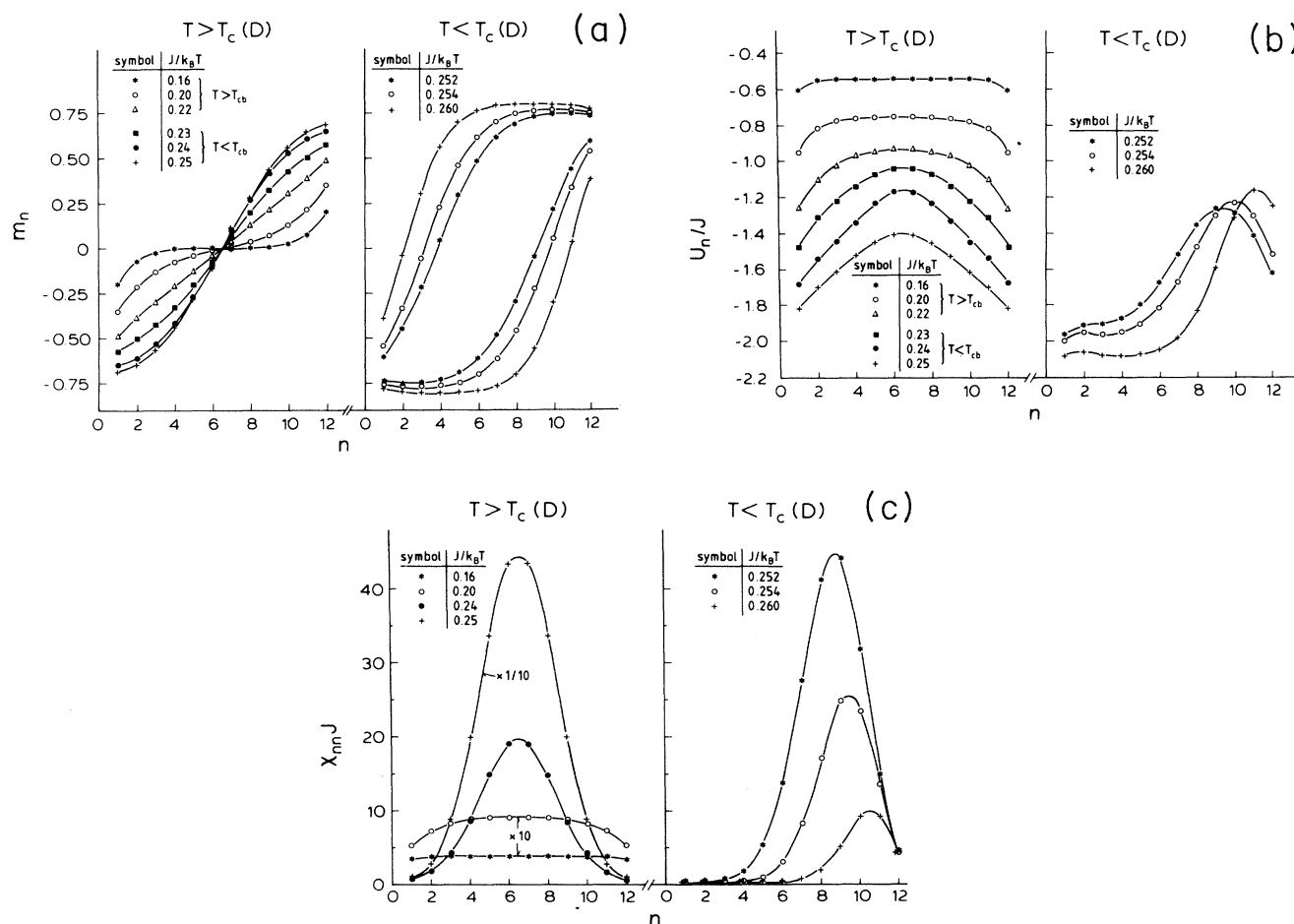$$m_n \propto -|H_1|\exp(-n/\xi_b), \quad n \ll D/2 , \tag{1}$$

FIG. 1. Profiles of the layer magnetizations $m_n(a)$, the normalized layer energies $U_n/J(b)$, where J is the nearest-neighbor exchange constant, and the layer susceptibilities $\chi_{nn}J(c)$ vs layer number n, for a thin film of thickness $D = 12$ (all lengths being measured in units of the lattice spacing of the simple cubic lattice), with surface fields $H_1/J = -0.55$, $H_D/J = +0.55$, and bulk field $H = 0$. The lateral linear dimension was chosen large enough (typically, $L = 128$ or 256) that for the temperatures shown, any effects on these profiles associated with the finiteness of L are negligible. The left-hand part of each panel shows data for temperatures T above the thin film critical temperature $T_c(D)$, the right-hand part shows data for three temperatures below $T_c(D)$ for which two states exist, one with positive total magnetization [upper three curves in (a)] and one with negative total magnetization [lower three curves in (a)]. For the sake of clarity, only the latter state is shown in (b) and (c). Curves through these profiles are drawn only as guides to the eye.

$$m_n \propto +|H_D|\exp\{-(D-n+1)/\xi_b\} \ ,$$

$$D-n+1 \ll D/2 \ , \qquad (2)$$

where ξ_b is the (true) correlation range of the bulk in a lattice direction for the three-dimensional Ising model, and all lengths are measured in units of the lattice spacing. Of course, Eqs. (1) and (2) are valid only as long as $\xi_b \ll D/2$, so that the two walls are essentially noninteracting and the profiles of all quantities of interest are essentially flat in the center of the film.

This behavior gradually changes, when $D \approx 2\xi_b$, i.e., near the bulk phase transition temperature, $T = T_{cb}$, where the two interfaces start to "feel" each other, the profile of m_n then deviates distinctly from an exponential decay. The energy profile no longer has any extended flat part, and the layer susceptibility profile χ_{nn} develops a pronounced peak in the center of the film. However, this change of behavior leading to the gradual buildup of an interface in the center of the film is completely smooth and does not imply any singularities; for finite D the transition that occurs at T_{cb} in the bulk system $(D \to \infty)$ is smeared out for all finite D, as will be discussed in more detail in later sections.

However, at a much lower temperature $T_c(D)$ (which for the present choice of surface field is already rather close to the wetting transition temperature of a semi-infinite system, $J/k_B T_W = 0.250 \pm 0.005$ for $|H_1|/J = 0.55$ [26]), one does observe symmetry breaking in the film: the interface between the phases with negative and positive magnetization is no longer located in the center of the film but is instead bound either to the left or to the right wall (for $H_1 = -H_D$ there is an exact degeneracy between these two states, of course). This interface localization-delocalization for $D \to \infty$ is predicted [5] not to converge toward T_{cb} but rather to the wetting transition temperature [27],

$$\lim_{D \to \infty} T_c(D) = T_W(H_1/J) \ . \qquad (3)$$

Note, however, that in spite of this property, Eq. (3), the transition at $T_c(D)$ is the only one to be observed in the thin film at all, and the antisymmetry of the profiles m_n in Fig. 1(a) for $T > T_c(D)$ with respect to the center of the film [the point $m_n = 0$ for $n = (D+1)/2$] implies that the total magnetization of the film is exactly zero for $T > T_c(D)$, i.e.,

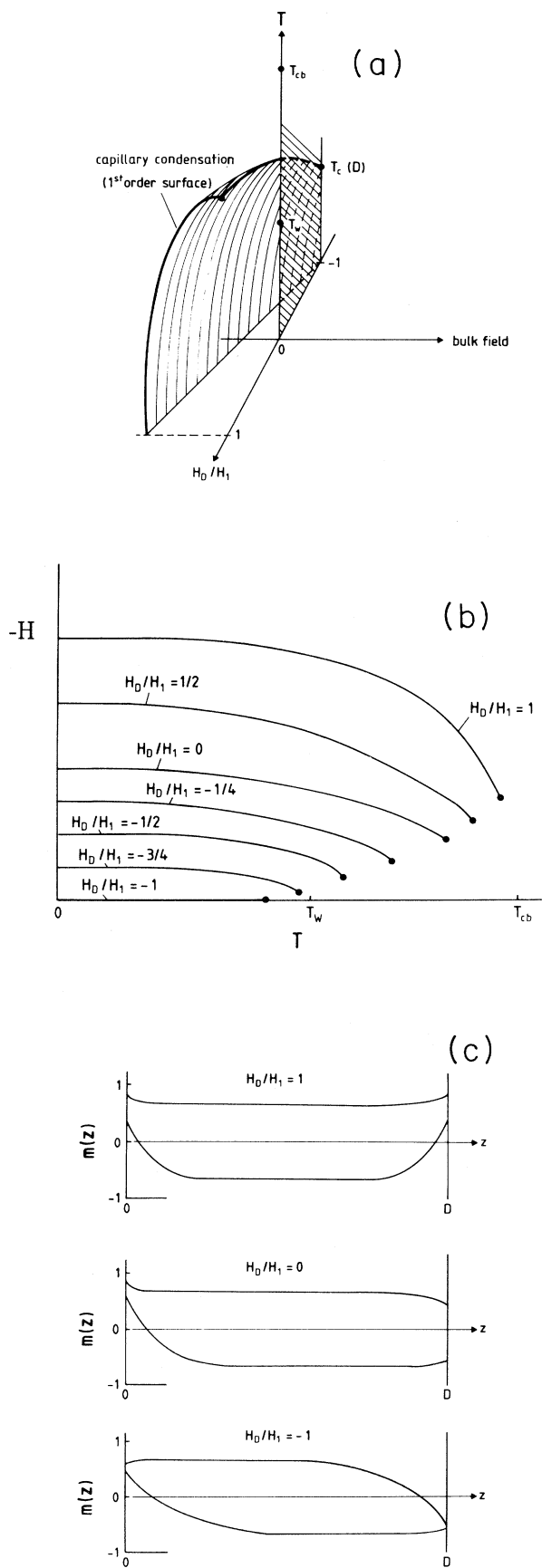$$\langle M \rangle = \frac{1}{D} \sum_{n=1}^{D} m_n = 0 \ . \qquad (4)$$

In contrast, the two states for $T < T_c(D)$ do have a spontaneous magnetization $M \neq 0$ of equal magnitude but opposite sign. Thus, focusing on the magnetization of the total film as the order parameter of the transition at $T_c(D)$, one notes a transition from a state where it is identically zero to a twofold degenerate state. Therefore, the resultant conclusion [5,9] is that the transition at $T_c(D)$ should belong to the universality class of the two-dimensional Ising model for all values of $D < \infty$. However, the proper theoretical description of phase transitions in this geometry is not completely clear [7,8].

Now, the situation with two walls with antisymmetric fields $H_D = -H_1$ certainly is very special, and it is not likely to be widely realized in physical fluid systems or mixtures, etc., where one rather expects the lack of any special symmetry or antisymmetry for inequivalent walls. Therefore, it is important to convince oneself that this transition, qualitatively described in Fig. 1, persists in the more general case of competing fields H_D/H_1 negative but $H_D \neq |H_1|$. A speculative attempt at such a generalization, which still awaits detailed verification, is presented in Fig. 2. The only distinction is that for $H_D/H_1 = -1$ the transition occurs exactly at zero bulk field, while for $H_D/H_1 > -1$ it occurs at nonzero bulk field—and then the two profiles coexisting with each other for $T < T_c(D)$ along the coexistence curve in the (H,T) plane are no longer antisymmetric images of each other. It is not an accident that this more general case is reminiscent of the situation for capillary condensation; actually, the standard model for capillary condensation where $H_D = H_1$ is simply another limiting case of the same general phase diagram. A general asymmetric situation where both fields H_D, H_1 have the same sign but unequal magnitude will be similar to the standard capillary condensation case, while a case where H_D/H_1 have the opposite sign but unequal magnitude will be similar to the situation shown in Fig. 1. The distinction between the two cases is that at the critical field H_{crit} (which depends on H_D/H_1, of course) the magnetization of the film is in general nonzero, with $M[H = H_{crit}, T = T_c(D)] = M_{crit}$. Since the order parameter at the transition is no longer symmetric around $M = 0$ it must instead be chosen as $M - M_{crit}$ and exhibits a symmetry only as $T \to T_c(D)$. The most important point is that when H_D and H_1 have different signs, we expect that $T_c(D)$ for $D \to \infty$ will lie in between $T_W(H_1/J)$ and $T_W(H_D/J)$ because $T_W(H_D/J = 0) = T_{cb}$ and the phase diagram has the same shape for all D as drawn in Fig. 2(a)—only the scale of the bulk field and of temperature distances from T_{cb} change.

Since standard capillary condensation $(H_D = H_1)$ has been studied elsewhere in great detail [14,20,21], we focus here on the strictly antisymmetric case $(H_D = -H_1)$, leaving a numerical investigation of the general asymmetric case to future work. In Sec. II, we briefly comment on the model and simulation technique, while Sec. III presents more data on profiles for different choices of the thickness D of the film. Section IV describes our attempts to establish the two-dimensional Ising character of the transition from a finite size scaling [11,28–30] analysis. Section V describes the anomalous behavior of the phase encountered for $T_c(D) < T \lesssim T_{cb}$, where the freely floating interface in the center of the film gives rise to very large response functions; (both χ_{nn} and the layer susceptibility $\chi_n = \partial m_n /\partial H$ vary exponentially with film thickness D, as predicted by Parry and Evans [9]). Finally, Sec. VI summarizes some conclusions.

II. MODEL AND SIMULATION TECHNIQUE

We study the Ising Hamiltonian on the simple cubic lattice in a $L \times L \times D$ geometry, applying periodic bound-

ary conditions in the x and y directions. At the two free $L \times L$ surfaces at layer numbers $n = 1$ and $n = D$, fields H_1 and H_D are applied:

$$\mathcal{H} = -J \sum_{\langle i,j \rangle} S_i S_j - H \sum_i S_i - H_1 \sum_{i \in \text{surface } 1} S_i$$

$$- H_D \sum_{i \in \text{surface } D} S_i, \quad S_i = \pm 1 . \tag{5}$$

In this work we confine ourselves to bulk field $H = 0$ and $H_D = -H_1$, with the restriction that $H_1/J = -0.55$, for which the wetting temperature has already been located, $k_B T_W/J \approx 4.00$ [26]. Thus, T_W lies sufficiently below T_{cb} [31], so that we are not affected by bulk critical fluctuations for T near T_W, but T_W also lies far away from the roughening transition temperature T_R ($k_B T_R/J = 2.445$ [32]). Of course, we do not expect that any of our results depend significantly on the precise value of H_1/J, and some less extensive calculations carried out for somewhat different choices of H_1/J confirm this expectation.

We implemented an efficient multispin coding single spin flip algorithm on an IBM ES/9000 vector computer facility as well as multilattice and standard Metropolis algorithms on IBM RISC workstations (with careful tuning to avoid cache computer memory problems). Since we deal with an inhomogeneous system and wish to consider temperatures over a wide range, from above T_{cb} to below $T_W(H_1/J)$, it is clear that standard cluster algorithms would offer no advantage. Moreover, cluster algorithms tailored to interface problems [33] were deliberately not implemented because we believe that the transition we want to study falls ultimately in the class of the bulk two-dimensional Ising model. Since our aim was to gain an overview of the system behavior for a wide range of temperatures and film thickness D, excessively large values of L were avoided. Typically, L varied from 32 to 128, but occasionally both smaller ($L = 16$) and larger ($L = 192$ or 256) sizes were used. Thicknesses studied were $D = 6$, $D = 8$, $D = 12$, and $D = 20$ (although the latter case was not investigated very systematically, since it would require an enormous amount of computing time). Even larger thicknesses (up to $D = 40$) were oc-

FIG. 2. (a) Qualitative phase diagram for a three-dimensional Ising film of thickness D with surface fields $H_1 > 0$ and H_D [for $H_1 < 0$ the phase diagram is the mirror image of the one shown with the (shaded) plane $H = 0$ as mirror plane]. There is a first-order surface of capillary-condensation transitions, ending in a line of capillary-condensation critical points $T_c(D;H_D/H_1)$. For $H_D/H_1 = -1$ this first-order surface occurs at $H = 0$ and $T_c(D,H_D/H_1 = -1) = T_c(D)$ is the location of the two-dimensional Ising-like transition considered in Eq. (3). (b) First-order capillary-condensation transitions (shown only qualitatively as lines ending in capillary condensation critical points (dots) for various choices of H_D/H_1. (c) Schematic order parameter profiles $m(z)$ at phase coexistence (in a continuum representation) plotted as a function of the distance z across the film for three values of H_D/H_1. The upper part is for "standard" capillary condensation, the middle part shows an arbitrary, asymmetric case, and the lowest part shows the antisymmetric situation studied in the present paper.
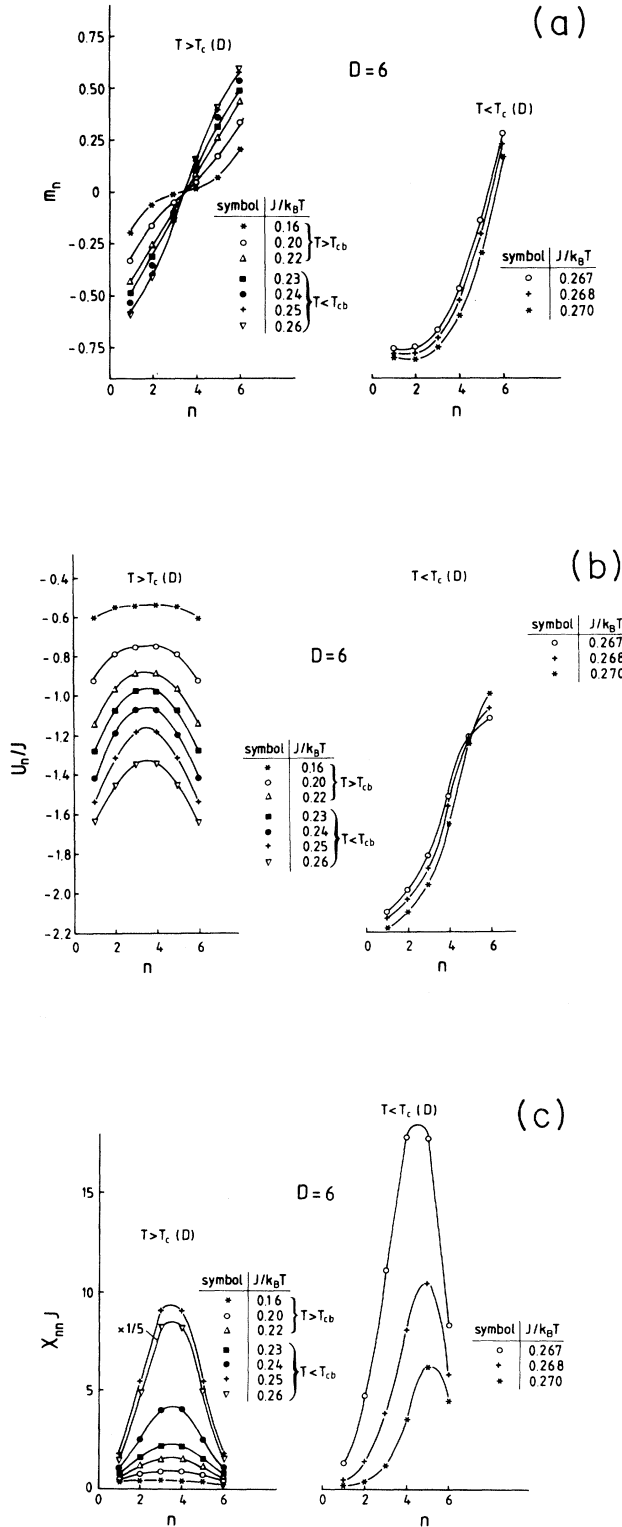
FIG. 3. Profiles of the layer magnetizations m_n (a), the normalized layer energies U_n/J (b), and the layer susceptibilities $\chi_{nn}J$ (c) plotted vs layer number n, for $D=6$, $L=128$, $H_1/J=-H_D/J=-0.55$, and various choices of inverse temperature. The mirror images of the profiles that occur below $T_c(D)$ for positive total magnetization have been omitted to simplify the figure.

casionally considered. However, one should not gauge these modest sizes by the linear dimensions that are now possible for standard critical phenomena: Note that in the present model we expect a nearly divergent correlation length $\xi_\parallel$ of the form $\xi_\parallel \propto \exp(D/4\xi_b)$ [9] over a broad range of temperature. Estimating that the critical slowing down will then be described by a correlation time $\tau \propto \xi_\parallel^z$, where z is the dynamic exponent ($z \approx 2$ [34]), we anticipate much more severe slowing down than in more standard models.

The quantities studied include profiles of magnetization m_n, energy U_n, and the layer susceptibilities χ_n and χ_{nn}. The latter were not obtained from the definitions quoted above, but rather from the fluctuation relations

$$\chi_{nn} = L^2(\langle \sigma_n^2 \rangle - \langle \sigma_n \rangle^2)/k_B T ,\tag{6}$$

$$\chi_n = L^2 D(\langle \sigma_n M \rangle - \langle \sigma_n \rangle\langle M \rangle)/k_B T ,\tag{7}$$
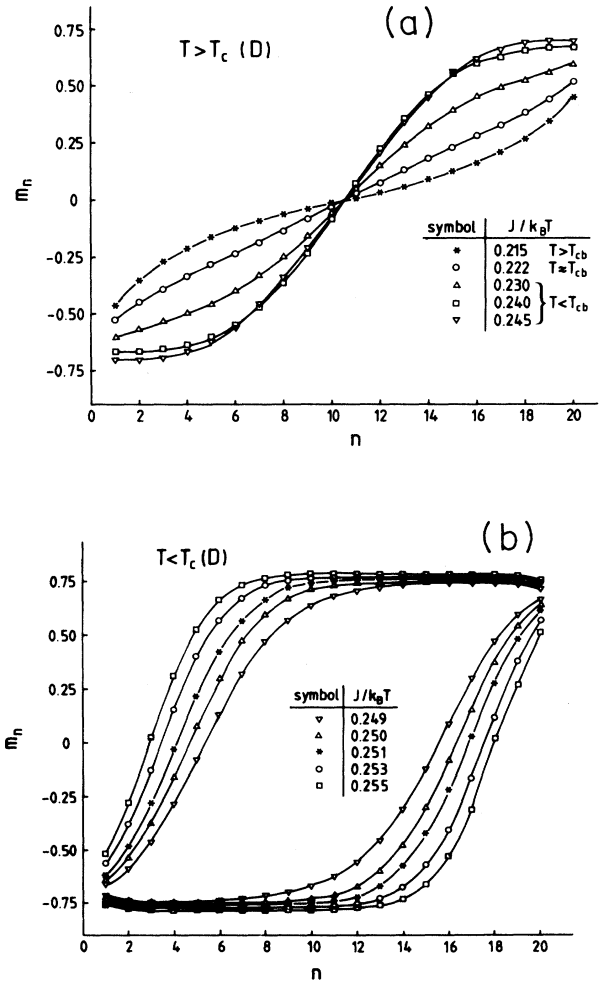
where

FIG. 4. Profiles of the layer magnetization m_n plotted vs layer number n for $D=20$, temperatures $T > T_c(D)$ (a), and $T < T_c(D)$ (b). Linear dimension L was $L=128$ throughout.

$$m_n = \langle \sigma_n \rangle, \sigma_n = \frac{1}{L^2} \sum_{i \in \text{layer } n} S_i, \quad M = \frac{1}{L^2 D} \sum_i S_i . \quad (8)$$

In addition, quantities characterizing the thin film as a whole have been calculated using the usual definitions [35]. This includes the total internal energy

$$E = \langle \mathcal{H} \rangle / (L^2 D) , \quad (9)$$

total specific heat

$$C = L^2 D (\langle \hat{\mathcal{H}}^2 \rangle - \langle \hat{\mathcal{H}} \rangle^2) / k_B T^2 , \quad \hat{\mathcal{H}} = \frac{\mathcal{H}}{L^2 D} \quad (10)$$

susceptibilities χ_{tot}, χ' appropriate above and below $T_c(D)$,

$$\chi_{\text{tot}} = L^2 D \langle M^2 \rangle / k_B T , \quad (11)$$

$$\chi' = L^2 D (\langle M^2 \rangle - \langle |M| \rangle^2) / k_B T , \quad (12)$$

as well as the reduced fourth-order cumulant U_L

$$U_L = 1 - \langle M^4 \rangle / (3 \langle M^2 \rangle^2) . \quad (13)$$

The typical length of runs was 2×10^5 Monte Carlo steps per site, although near $T_c(D)$ considerably longer runs were also carried out, particularly for the larger choices of L. However, due to the dramatic critical slowing down occurring in this model, the data were often found to be too strongly correlated to allow a decent analysis of statistical errors. In such cases we have carried out several independent runs with different random numbers to get more reliable estimate of the inaccuracies. Because most of the figures in the following sections contain so many data points, we have chosen to include error bars in only a few data plots and in some figures showing analyses. In most cases, the error bars for the order parameter and energy are smaller than the size of the symbols; the errors in the fluctuation quantities, e.g., susceptibilities and specific heats, are often larger.
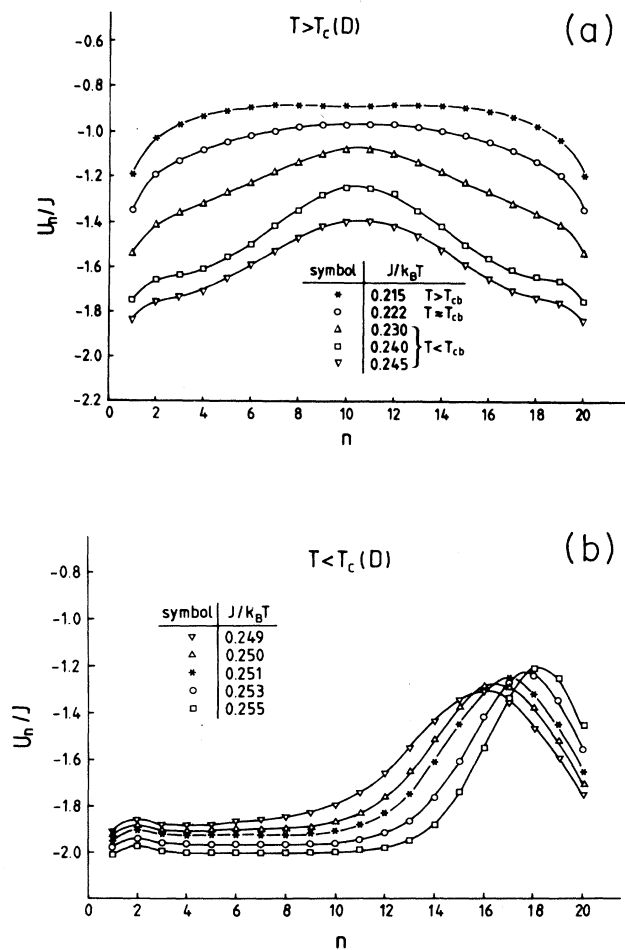
For studies of wetting, layering, and surface critical

FIG. 5. Profiles for the layer energy U_n/J plotted vs layer number n for $D = 20$, temperatures $T > T_c(D)$ (a), and $T < T_c(D)$ (b). The mirror images of the profiles that occur below $T_c(D)$ for positive total magnetization have been omitted to simplify the figure.
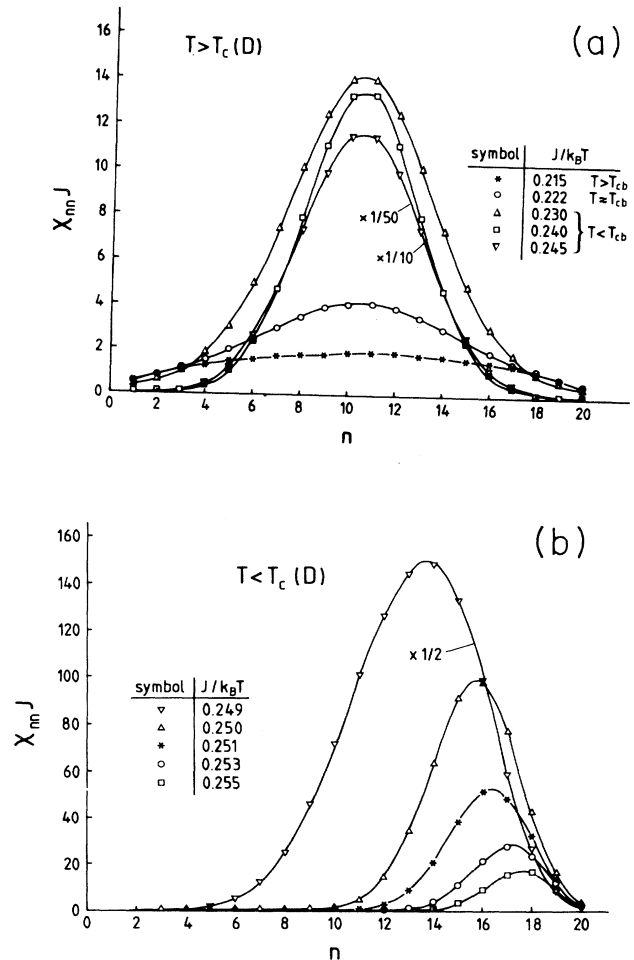
FIG. 6. Profiles of the layer susceptibility $\chi_{nn} J$ plotted vs layer number n for $D = 20$, temperatures $T > T_c(D)$ (a), and $T < T_c(D)$ (b). The mirror images of the profiles that occur below $T_c(D)$ for positive total magnetization have been omitted to simplify the figure.

phenomena [26,36–38], we have found it useful to consider sites near the free surfaces more often for a spin flip than sites in the bulk ("preferential surface site selection"). Here the situation is reversed; the surface fields suppress fluctuations in the layers close to the surfaces, and the largest and slowest fluctuations occur in the center of the film due to the fluctuating interface. Therefore, in the present work, the inverse of preferential surface site selection was implemented: Typically, sites in the center of the film were visited four times more often than sites near the walls.

III. PROFILES FOR SEVERAL THICKNESSES

In Fig. 1 we have already presented some profiles for a thin film of thickness $D=12$. Since it is of great interest to check how this behavior varies with thickness, we discuss additional profiles for $D=6$ and $D=20$ (profiles for $D=8$ have also been recorded, but are omitted here in order to save space, as they are rather similar to those for $D=6$).

Figure 3 shows the data for the thinnest film that was studied, $D=6$. Comparing those data to those in Fig. 1, we note that even far above T_{cb} (e.g., for $J/k_B=0.20$) the profiles of order parameter and energy are not flat, unlike the case $D=12$. This is easy to understand, since the smaller D becomes, the smaller the bulk correlation length ξ_b must be to render interactions between the two walls negligible. Similarly, while for $D=12$ and $T<T_c(D)$ the order parameter profile quickly develops a flat region where m_n is quite close to its value in a bulk three-dimensional system, no such behavior can be identified here. While for $D=12$ one can already speak of the picture where a well developed interface bound to either of the walls separates bulk phases of negative or positive magnetization, no separation between "interface" and "bulk phases" is possible for films as thin as $D=6$. For such thin films, all layers feel the effects of the two competing walls rather strongly. Thus, it was clear that little could be learned by choosing thicknesses even smaller than $D=6$, although such systems clearly would be relatively easy to simulate.

As expected, a rather different picture emerges for $D=20$ (Figs. 4–7). For $T>T_{cb}$ the two walls only start to interact very close to the critical point, and for $T_c(D)<T<T_{cb}$ one recognizes rather clear bulk behavior in a region near the walls, separated by a broad interface in the center of the film. This interface shows up via clear peaks in the layer energy and the layer susceptibility χ_{nn}. Note also that this latter quantity now reaches much larger values than for $D=6$ [Fig. 3(c)] and $D=12$ [Fig. 1(c)]. This is already a qualitative indication of the anticipated exponential divergence of χ_{nn} with film thickness for $T_c(D)>T>T_{cb}$, which will be analyzed in more detail in Sec. V.

A satisfactory picture also emerges from a study of the profiles in the region for $T<T_c(D)$, where we expect the interface separating bulk three-dimensional phases to be bound either to the right or to the left wall. Figure 4(b) gives clear evidence of this description, and one can see how the interface increasingly "depins" from the surface as T approaches $T_c(D)$ from below.
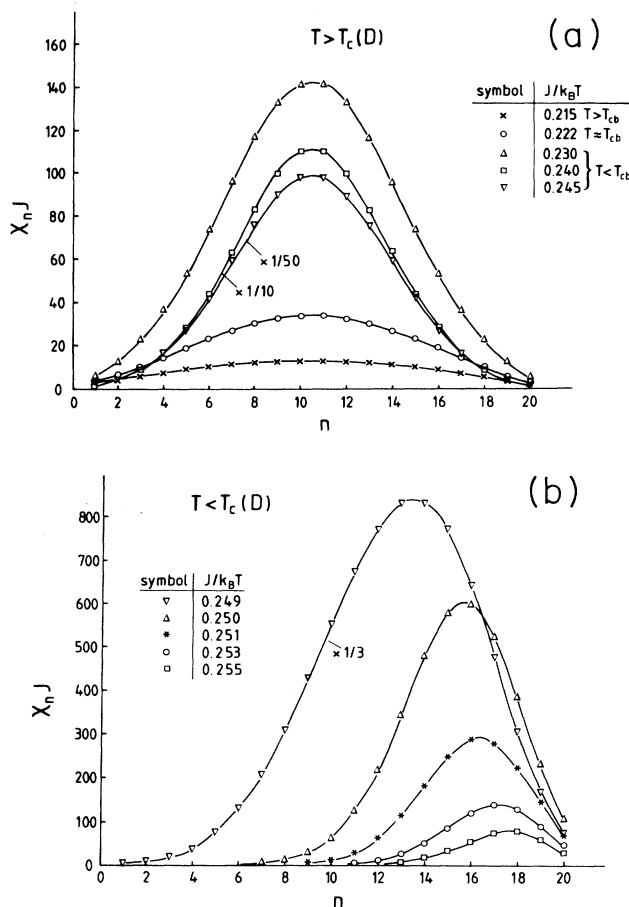

FIG. 7. Profiles of the layer susceptibility $\chi_n J$ plotted vs layer number n for $D=20$, temperatures $T>T_c(D)$ (a), and $T<T_c(D)$ (b). The mirror images of the profiles that occur below $T_c(D)$ for positive total magnetization have been omitted to simplify the figure.
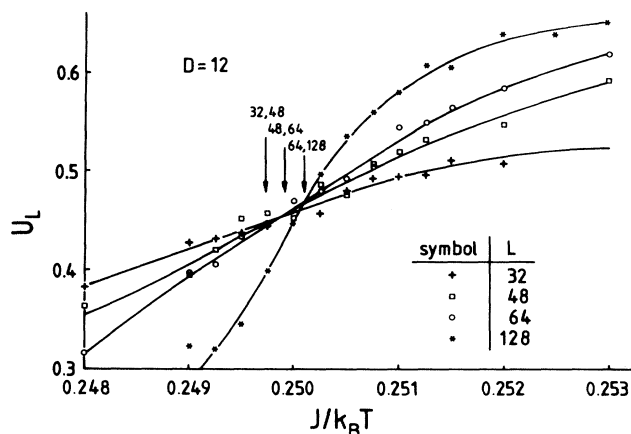

FIG. 8. Cumulants U_L [Eq. (13)] plotted vs inverse temperature for $D=12$, $|H_1|/J=0.55$, and several choices of L. The arrows indicate the locations of cumulant crossings of pairs of sizes. Note that $J/k_B T_W \approx 0.250$ for $|H_1|/J=0.55$ and that the bulk Ising transition at $J/k_B T_{cb} \approx 0.227$ is far off scale. Curves are only guides to the eye.

IV. FINITE SIZE SCALING ANALYSIS
OF THE PHASE TRANSITION AT $T_C(D)$

First we attempted to locate the transition for $D = 12$ from the cumulant crossings for different sizes (Fig. 8). For $L \leq 64$ one indeed finds a well defined intersection point at $J/k_B T \approx 0.2497$, rather close to the corresponding wetting transition temperature [26], compatible with Eq. (3). However, the data exhibit two disturbing features: (i) the ordinate U^* of this cumulant crossing is rather close to $U^* \approx 0.45$, rather than to the value U^* (2D Ising) ≈ 0.615 characterizing the universality class of the two-dimensional Ising model [39]; (ii) the data for $L = 128$ seem to yield a decidedly different intersection point that occurs at a somewhat higher temperature and at a slightly larger value $U^* \approx 0.47$.

The behavior of other quantities is also somewhat unusual: the specific heat [Fig. 9(a)] has only a very weak

anomaly (those for $L = 32\text{–}64$ can hardly be distinguished from each other with a more pronounced increase beginning only for $L = 128$); the susceptibility χ for temperatures far above $T_c(D)$ is roughly compatible with two-dimensional Ising behavior [Fig. 9(b)], but the finite size rounding of this anomaly near $T_c(D)$ does not scale with the two-dimensional Ising exponents. (The precise estimation of $T_c(D)$ will be discussed below.) A plot of the order parameter $\langle |M| \rangle$ [Fig. 9(c)], however, reveals behavior that seems incompatible with two-dimensional Ising criticality.

A possible resolution to this puzzle becomes likely when we recall the prediction of a very large lengthscale $\xi_\parallel \propto \exp(D/4\xi_b)$ [9] in the phase with the delocalized interface [$T_c(D) < T < T_{cb}$]. It is then likely that the true nature of the transition can be observed only when L is clearly larger than $\xi_\parallel$. In fact, we can expect that a large
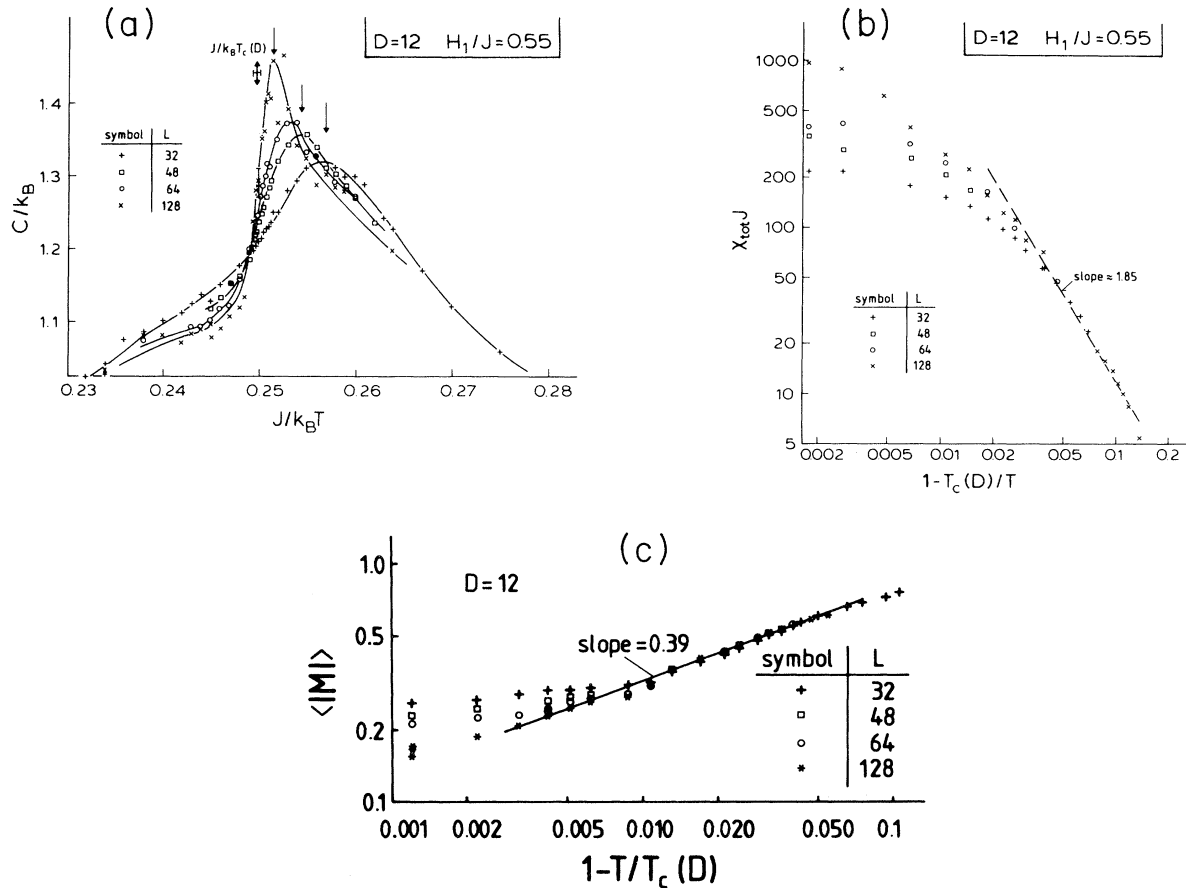

FIG. 9. (a) Specific heat per spin C/k_B plotted vs inverse temperature for films of thickness $D = 12$, $|H_1|/J = 0.55$, and three linear dimensions L as indicated. Arrows indicate the estimated locations of the specific heat maxima, while the double arrow indicates the estimate of $T_C(D)$ that resulted from the cumulant crossings. (b) Log-log plot of the susceptibility $\chi_{\text{tot}} J$ vs the reduced temperature distance $1 - T_c(D)/T$ for $T > T_c(D)$, $D = 12$, and $|H_1|/J = 0.55$. Four lattice sizes L are included as shown. At high temperatures the data are compatible with a law $\chi \propto [1 - T/T_c(D)]^{-\gamma_{\text{eff}}}$, with $\gamma_{\text{eff}} \approx 1.85$, as indicated by the broken straight line, roughly compatible with the expected Ising behavior [$\gamma(d = 2) = 1.75$]. Here, $J/k_B T_c(D) \approx 0.2497$ was used. (c) Log-log plot of the order parameter $\langle |M| \rangle$ vs the reduced temperature distance $1 - T/T_c(D)$ for $T < T_c(D)$, $D = 12$, and $|H_1|/J = 0.55$. At $0.01 \lesssim 1 - T/T_c(D) \lesssim 0.06$ the data are compatible with a law $\langle |M| \rangle \propto [1 - T/T_c(D)]^{-\beta_{\text{eff}}}$, with $\beta_{\text{eff}} \approx 0.39$, as indicated by the solid line, and incompatible with the expected Ising behavior [$\beta(d = 2) = 0.125$]. Here, $J/k_B T_c(D) \approx 0.2497$ was used.
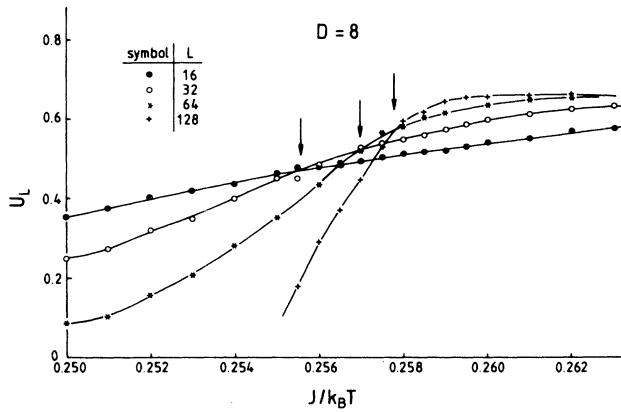
FIG. 10. Cumulants U_L [Eq. (13)] plotted vs inverse temperature for the case $D=8$, $|H_1|/J=0.55$, and several choices of L as indicated. The arrows indicate the locations of cumulant crossings of two neighboring lattice sizes.

$\xi_\parallel$ leads to a large critical amplitude $\hat{\xi}$ when we approach the Ising transition, where the correlation length must diverge,

$$\xi = \hat{\xi}_\pm |1 - T/T_c(D)|^{-\nu}, \quad \nu(d=2)=1 . \quad (14)$$

Here, the two signs of the critical amplitude refer to temperatures above $(\hat{\xi}_+)$ and below $(\hat{\xi}_-)T_c(D)$, respectively. The large value of the critical amplitude implies that the asymptotic region of the two-dimensional Ising critical behavior is very narrow. For choices of L such that $L \lesssim \xi_\parallel$, the interfacial fluctuations are not yet restricted significantly by the finite thickness of the film; instead one has finite size rounding of the wetting transition due to the finiteness of L and can treat the film thickness as quasi-infinite. Since at $J/k_B T = 0.25$ the true correlation length is expected to be only of the order of one lattice spacing $(\xi_b \approx 0.92$ [40,41]), for $D=12$ the factor $\exp(D/4\xi_b) \approx 26$ and hence the regime $L \gg \xi_\parallel$ is not
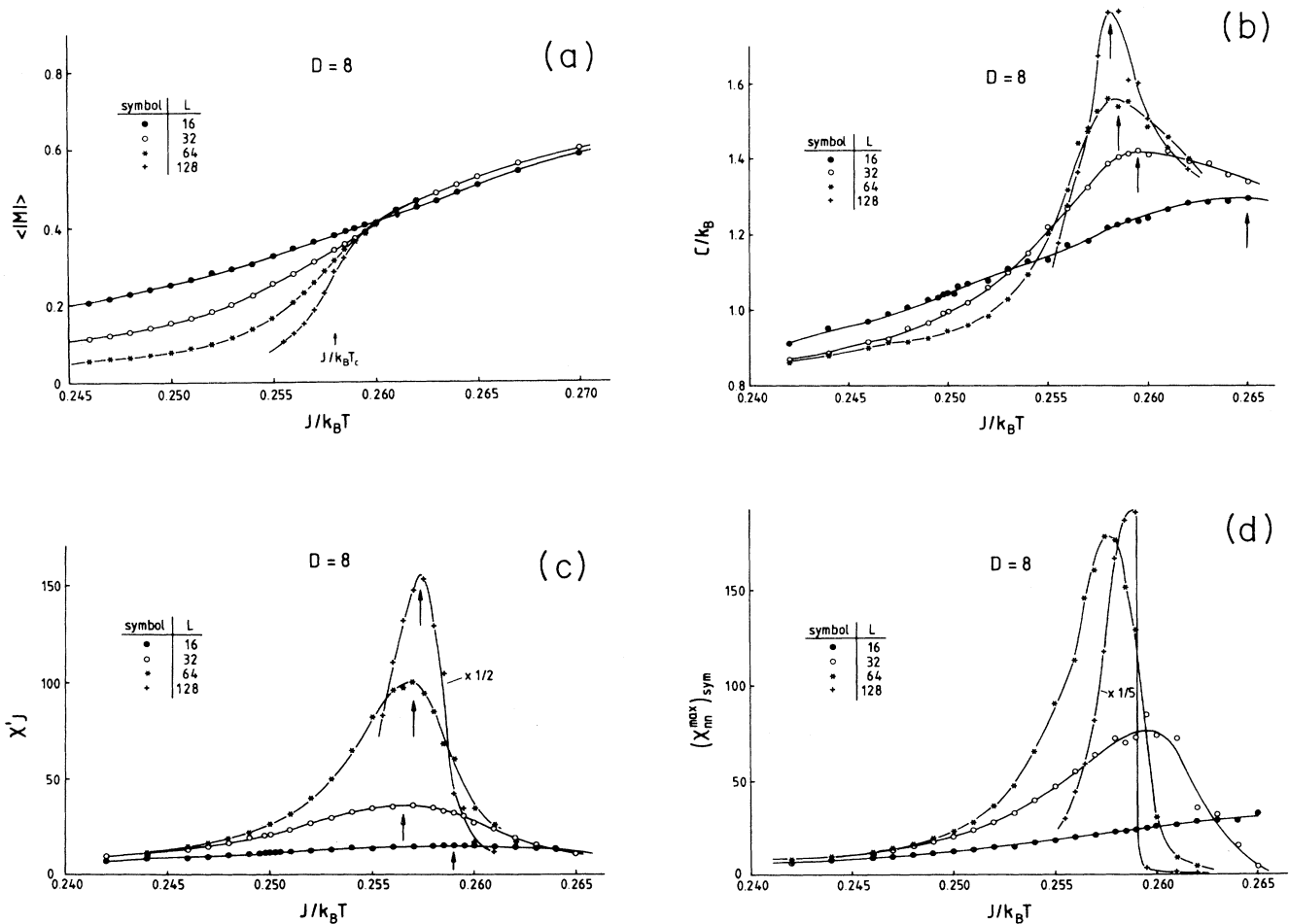

FIG. 11. Order parameter $\langle |M| \rangle$ (a), specific heat C/k_B (b), suseptibility $\chi' J$ (c), and maximum value of the layer susceptibility $\chi_{nn}^{max} J$ (d) plotted vs inverse temperature for $D=8$. Several sizes of L are included as indicated.

reached for our smaller choices of L. In view of this consideration, smaller thicknesses, such as $D=8$ and $D=6$ [for which the factor $\exp(D/4\xi_b)=8.8$ ($D=8$) or 5.1 ($D=6$)] become interesting.

In Figs. 10–13 we show data for $D=8$. Now the cumulant crossings are spread out even more distinctly (Fig. 10), indicating that for $D=8$ we have fully entered a crossover region. Note that for this small thickness, $T_c(D)$ (which can be estimated by extrapolating the temperatures of the cumulant crossings to $L \to \infty$; see Fig. 12 below) now occurs at a temperature distinctly lower than $T_W(H_1)$.

Figure 11 shows that the specific heat maximum is still very shallow and broad for $L \leq 32$, whereas for $L=128$ a rather pronounced peak develops. With increasing L the location of this peak shifts systematically to higher temperature [Fig. 11(b)], while for $L \geq 32$ the peak position of χ' shifts to lower temperature [Fig. 11(c)]. These data are thus suitable for an extrapolation to $L \to \infty$ (Fig. 12), while the behavior of the layer susceptibility maximum [Fig. 11(d)] is less monotonic and hence not so well suited for an extrapolation.

Figure 12 shows that the data for the temperatures $T_{U\,\mathrm{cross}}$ of the cumulant crossings, the temperatures of the

FIG. 13. Log-log plot of the maxima value of the susceptibility $(\chi'J)_{max}$ vs L. Also, data for the total susceptibility $(\chi_{tot}J)_{T_c(D)}$ are included. Straight lines indicate an effective exponent $(\gamma/\nu)_{eff} \approx 1.7$, which is not far off the theoretical two-dimensional Ising value $\gamma/\nu=1.75$.

maxima of specific heat $(T_{C_{max}})$ and susceptibility $(T_{\chi'_{max}})$ are roughly compatible with a linear extrapolation in the variable L^{-1}, yielding $J/k_BT_c(D)=0.2578\pm0.0002$. Note that the "natural" extrapolation should use a variable $L^{-1/\nu}$, with $\nu=1$, the value of the two-dimensional Ising model, as $L \to \infty$. It is not obvious that such an extrapolation should already work in the crossover regime
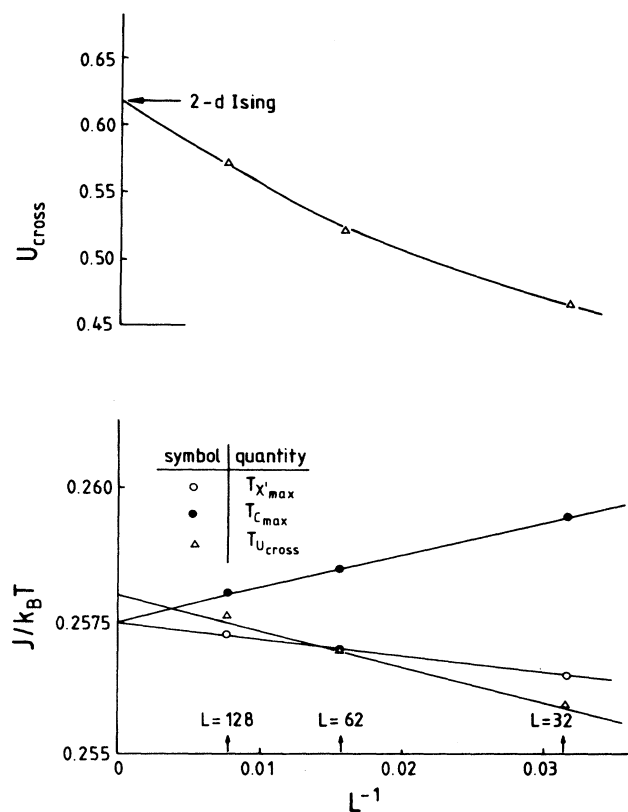

FIG. 12. Extrapolation of the values of the cumulant crossings U^* vs L^{-1} (upper part) and extrapolation of the inverse temperatures of these crossing points as well as the inverse temperatures of the specific heat and susceptibility maxima vs L^{-1}. The arrow in the upper part shows the value of two-dimensional Ising criticality, $U^* \approx 0.615$ [39].
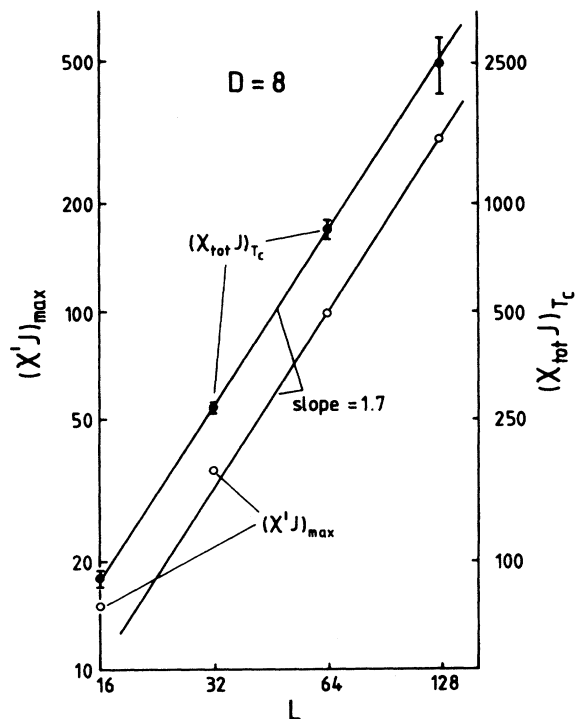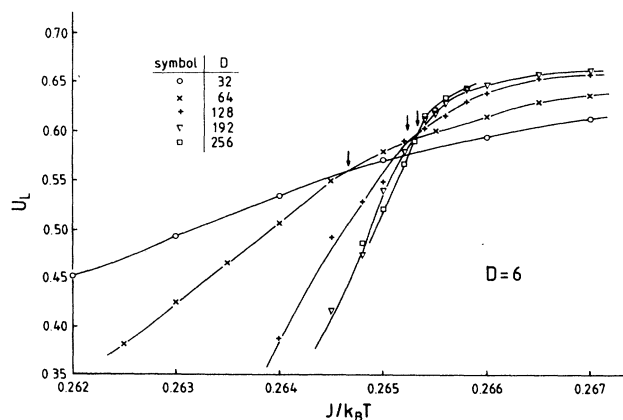

FIG. 14. Cumulants U_L [Eq. (13)] plotted vs inverse temperature for the case $D=6$, $|H_1|/J=0.55$, and several choices of L as indicated. The arrows indicate the locations of cumulant crossings of two neighboring lattice sizes.

where L is not yet much larger than $\xi_{\parallel}$. However, for a critical wetting transition described by mean field theory we also expect a correlation length exponent $\nu_{\parallel} = 1$ [15], and it is hence plausible that an extrapolation which is linear in L^{-1} works over a wide range of L. We attribute the scatter in the extrapolated values to the obvious inaccuracy in locating the temperatures $T_{C_{max}}$, $T_{\chi'_{max}}$ where specific heat and susceptibility χ' have their maxima because of the considerable statistical noise of the data in
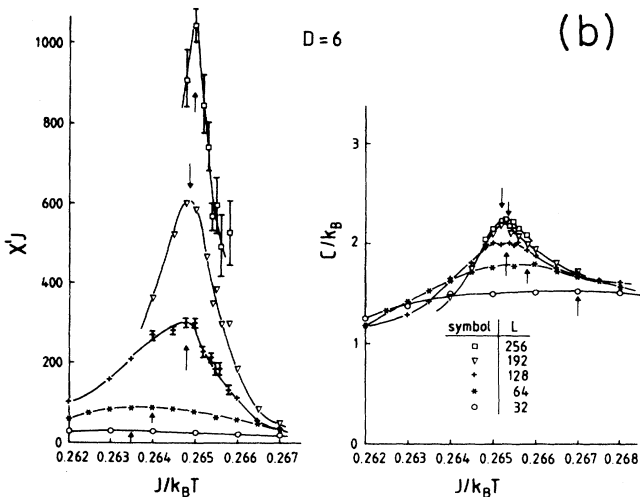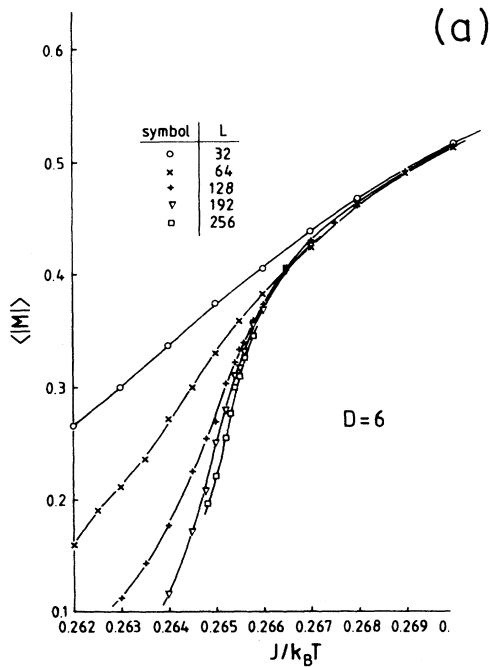

(a)

D = 6

(b)

FIG. 15. Order parameter $\langle |M| \rangle$ (a), susceptibility $\chi'J$ and specific heat C/k_B (b) plotted vs inverse temperature J/k_BT. Arrows in (b) show the estimates of temperatures $T_{c_{max}}$, and $T_{\chi_{max}}$ of specific heat and susceptibility maxima. A few error bars are shown near the transition; for small systems and away from the maxima, errors are smaller than the size of the symbols.
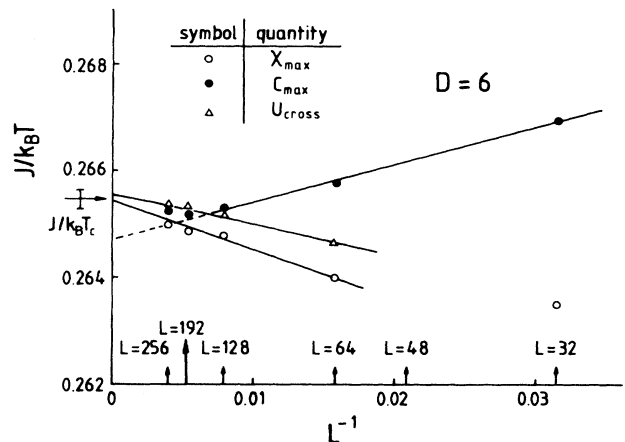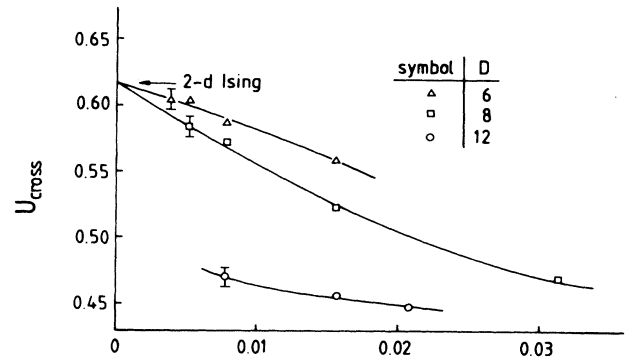
Fig. 11. What is more gratifying, of course, is the smooth extrapolation of the cumulant intersections $U_{cross}(L)$, defined from $U(L) = U(L/2) \equiv U_{cross}(L)$, toward the expected two-dimensional Ising value $U^* = 0.615$ [39]; see Fig. 12. The increasing of the susceptibility maxima with the linear dimensional L (Fig. 13) is also compatible with the expected finite size scaling behavior $[(\chi'J)_{max} \propto L^{\gamma/\nu}$ with $\gamma/\nu = 1.75$ for the two-dimensional Ising model].

These admittedly tentative conclusions are strengthened by the behavior of the thinnest film $(D = 6)$, shown in Figs. 14–18. While the intersection for the smallest sizes (32,64) in the cumulant intersection plot (Fig. 14) still suffers from crossover effects, the intersections for all the larger sizes converge rather nicely to the Ising value $(U^* = 0.615)$ with a spread in temperature which is also fairly small. The order parameter [Fig. 15(a)] rises much more steeply with decreasing temperature, which is indicative of the exponent $\beta = \frac{1}{8}$ of the two-dimensional Ising model. Both susceptibility χ' and specific heat C have

FIG. 16. Cumulant crossing values U_{cross} vs L^{-1} (upper part) for $D = 6$, 8, and 12. Arrows show the value of the 2D Ising universality class. Curves are only guides to the eye. Lower part shows for $D = 6$ the extrapolations of the temperatures $T_{U_{cross}}$ of cumulant intersections as well as of the susceptibility maxima $(T_{\chi'_{max}})$ and of the specific heat maxima. Arrow (with error bars) marks the final estimate of $J/k_BT_c(D) = 6$, while straight lines indicate possible extrapolations.

rather well developed peaks, and an extrapolation of their locations (Fig. 16) yields a value of $T_c(D)$ $[J/k_B T_c(D) = 0.2655 \pm 0.0002]$, which is compatible with the cumulant extrapolation. It must be noted, however, that the specific heat takes on its limiting behavior only
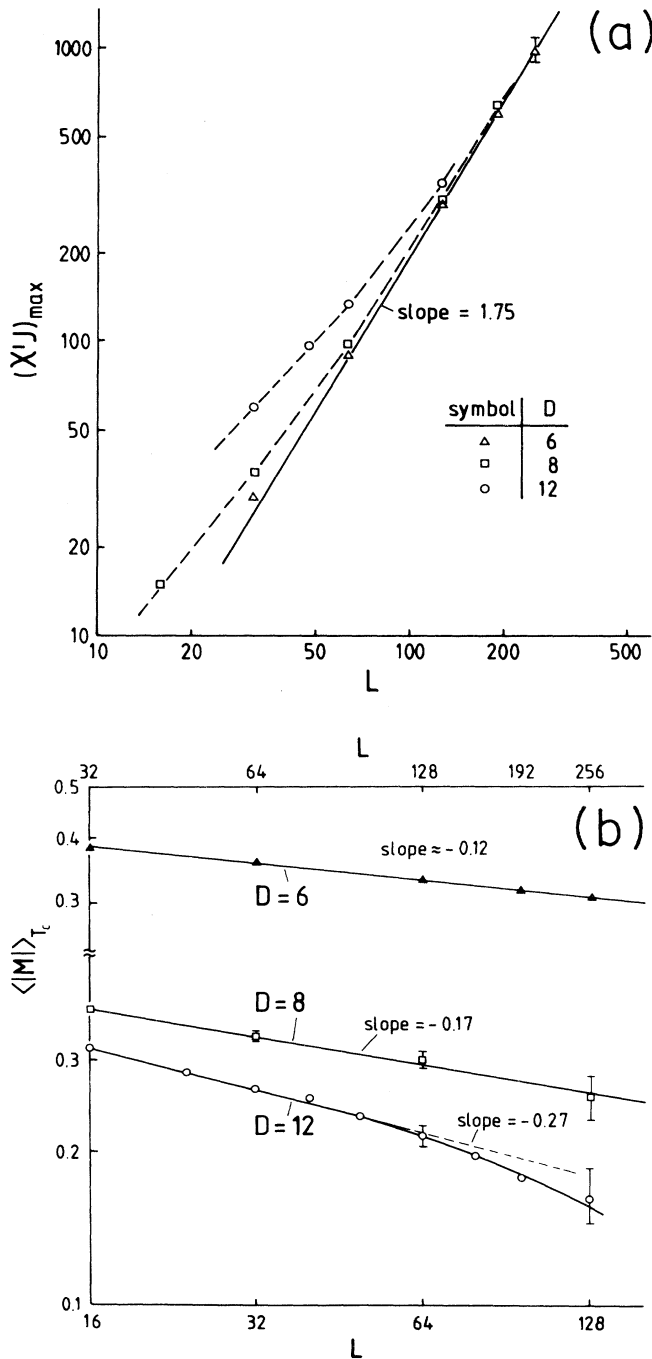
FIG. 17. Log-log plots of the maximum value of the susceptibility $(\chi' J)_{max}$ (a) and the order parameter $\langle |M| \rangle_{T_c}$ (b) vs L, including data for $D = 6$, 8, and 12. Only for $D = 6$ is the Ising behavior $(\chi' \propto L^{\gamma/\nu}$ with $\gamma = 1.75$, $\langle |M| \rangle_{T_c} \propto L^{-\beta/\nu}$ with $\beta/\nu = 0.125)$ clearly seen, while for larger D there is curvature and one can extract only "effective exponents."

for the largest sizes. In Fig. 16 we have also included an extrapolation of the values U_{cross} observed at these cumulant crossings, also extrapolating them as function of $1/L$, and comparing them to the corresponding values for $D = 8$ and $D = 12$. From this plot it is clear that extremely large values of L would be needed for $D = 12$, to come as close to the asymptotic 2D Ising behavior as for $D = 6$. The same conclusion results from a finite size analysis of the susceptibility maximum and $\langle |M| \rangle$ (Fig. 17).

Of course, many other quantities can be (and have been) analyzed. As an example, Fig. 18 shows the internal energy per spin, which is very smooth with hardly any anomaly at $J/k_B T_c(D)$, consistent with the weak specific heat peaks. The physical reason why only such a weak anomaly occurs at this Ising transition is that only the configurational entropy of the interface is affected by the interface localization-delocalization transition at $T_c(D)$, while away from the interface the system is already a well ordered Ising ferromagnet!

V. EVIDENCE OF AN EXPONENTIAL VARIATION OF SUSCEPTIBILITIES WITH FILM THICKNESS

The state of the film in the regime between $T_c(D)$ and T_{cb} is rather anomalous for large D: The system is essentially already ordered locally everywhere except in the immediate vicinity of the interface, which, on average, is located in the center of the film (Figs. 1 and 4). If the confining walls were an infinite distance from the center of the film, we would have a freely floating interface that could be shifted as a whole without free energy cost. For finite thicknesses $D \gg \xi_b$, this free energy cost is no longer strictly zero, but it is exponentially small in the ratio $D/(2\xi_b)$, at least in mean field theory [9]. These free energy costs of order $\exp\{-D/(2\xi_b)\}$ can be understood from the fact that in mean field theory the interface is not rough, and described by the familiar tanh profile,
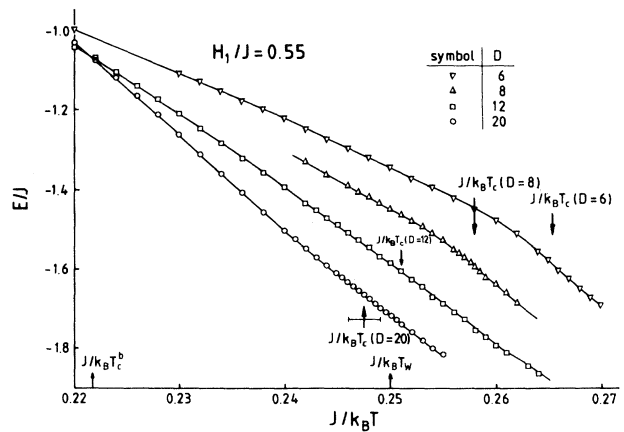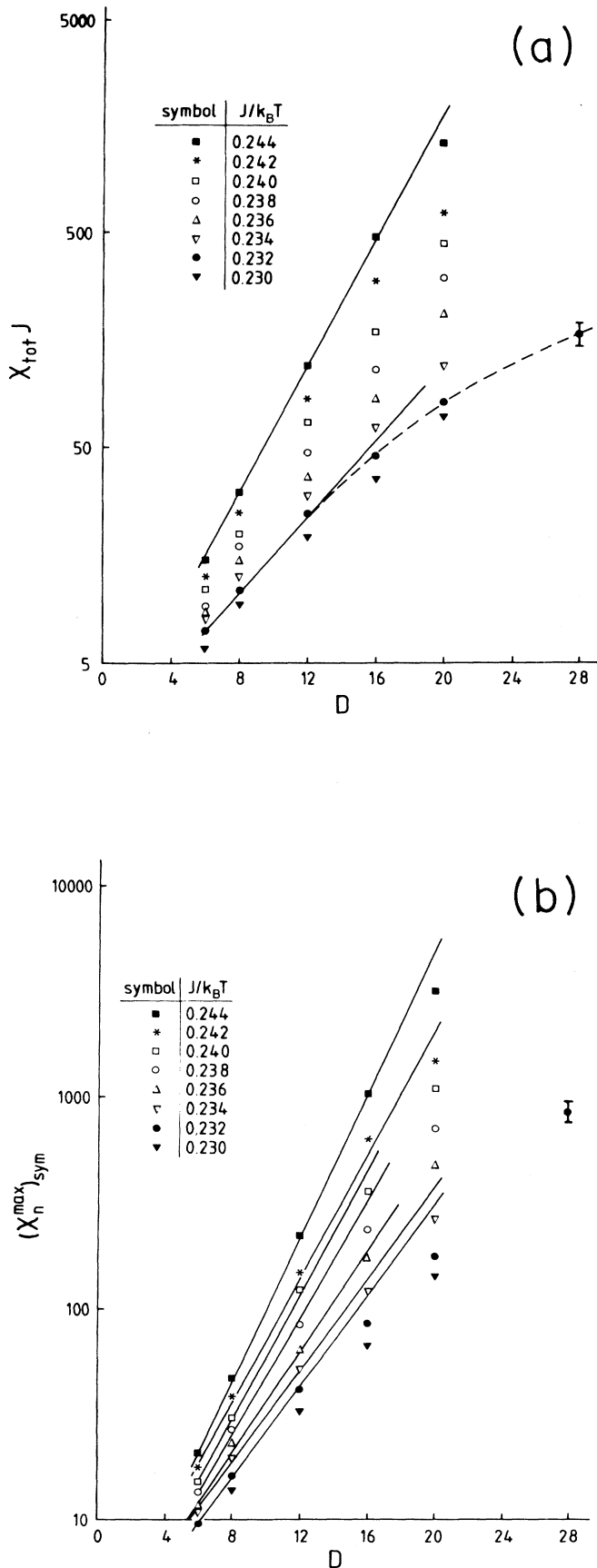
FIG. 18. Internal energy per spin E/J plotted vs inverse temperature for all the film thicknesses studied. Arrows show the estimates for the critical temperature $T_c(D)$, obtained from the extrapolation of cumulant intersections. Note that for $D = 20$ only a very rough estimate was feasible $[J/k_B T_c(D) = 0.2475 \pm 0.0015]$.

(a)

symbol	J/k_BT
■	0.244
✳	0.242
□	0.240
○	0.238
△	0.236
▽	0.234
●	0.232
▼	0.230

(b)

symbol	J/k_BT
■	0.244
✳	0.242
□	0.240
○	0.238
△	0.236
▽	0.234
●	0.232
▼	0.230

$$m(z) \approx -m_b \tanh(z/l) \ , \quad l = 2\xi_b \ , \quad (15)$$

where we take the zero of the z coordinate in the center of the interface. The intrinsic width $l/2$ is simply identical to the true correlation range in the direction perpendicular to the interface. Of course, Eq. (15) does not hold near $z \approx \pm(D-1)/2$ because the tanh profile at the walls is somewhat distorted due to the response to the surface fields $\pm H_1$. According to mean field theory [9], the free energy cost due to this weak distortion of the profile is of order $\exp\{-D/(2\xi_b)\}$. The application of fields H uniformly in the bulk to induce a magnetization (or a local field H_n in the nth layer, respectively) implies a displacement of the interface and, therefore, the response to these fields is also predicted to scale in proportion to the inverse of the above energy cost [9]:

$$\chi_n \propto \chi_{nn} \propto \exp\{D/(2\xi_b)\} \ , \quad D/\xi_b \gg 1 \ . \quad (16)$$

Figures 19 and 20 present a test of these predictions (for their detailed derivation, see Parry and Evans [9]; the above comments provide only a plausibility argument). Indeed, one sees that the data are roughly compatible with an exponential variation in thickness, but at the same time the mild curvature in Fig. 19 indicates that there are possibly pre-exponential corrections in Eq. (16). Therefore, a more stringent test of Eq. (16) is to plot $\ln(J\chi_n^{\max})_{\mathrm{sym}}/D$ and $\ln(J\chi_{nn}^{\max})_{\mathrm{sym}}/D$ versus D and $1/D$, respectively (Fig. 20). We see that $\ln(J\chi_{nn}^{\max})_{\mathrm{sym}}/D$ settles down nicely at a plateau in the available range of thicknesses, while for $\ln(J\chi_n^{\max})_{\mathrm{sym}}/D$ there is a pronounced decrease over the entire range of D studied [Figs. 20(a) and 20(b)]. However, if we extrapolate $\ln(J\chi_n^{\max})_{\mathrm{sym}}/D$ versus $1/D$, the limiting values l^{-1} of the interfacial length l defined via this analysis agree with the analysis of $\ln(J\chi_{nn}^{\max})_{\mathrm{sym}}/D$, Fig. 20(c). The slower approach of $\chi_n^{\max}$ to its limiting behavior can be understood when we compare the profiles for χ_n and χ_{nn} at $T > T_c(D)$ [see Figs. 6(a) and 7(a)], while for $D = 20$, χ_{nn} is essentially flat near the walls, and so the peak of χ_{nn} in the center of the film has possibly reached its limiting shape expected for large D. The lack of flatness in χ_n near the walls is evidence that the limiting shape has not yet been reached.

A rather unexpected feature of our results is the finding that the length l disagrees with the prediction of mean field theory, $2\xi_b$ [Fig. 20(a)]. Here, ξ_b, of course, was not calculated from molecular field theory but rather

FIG. 19. Semilog plots of the total susceptibility (a) and the maximum value of the layer susceptibility $(J\chi_n^{\max})_{\mathrm{sym}}$ (b) vs the film thickness D at various temperatures. Here the index "sym" means that the profile was symmetrized, i.e., $(\chi_n)_{\mathrm{sym}} = (\chi_n + \chi_{D+1-n})/2$, in order to smooth out the slow fluctuations in the interfacial position. Solid lines are drawn to indicate the extent to which the data are compatible with an exponential variation, and the broken curve is only a guide to the eye. Note that a few data points are shown for $D = 28$ but these may suffer from uncertainties in their statistical and systematic errors (finiteness of L) and are included only to show that no surprises occur at large values of L.
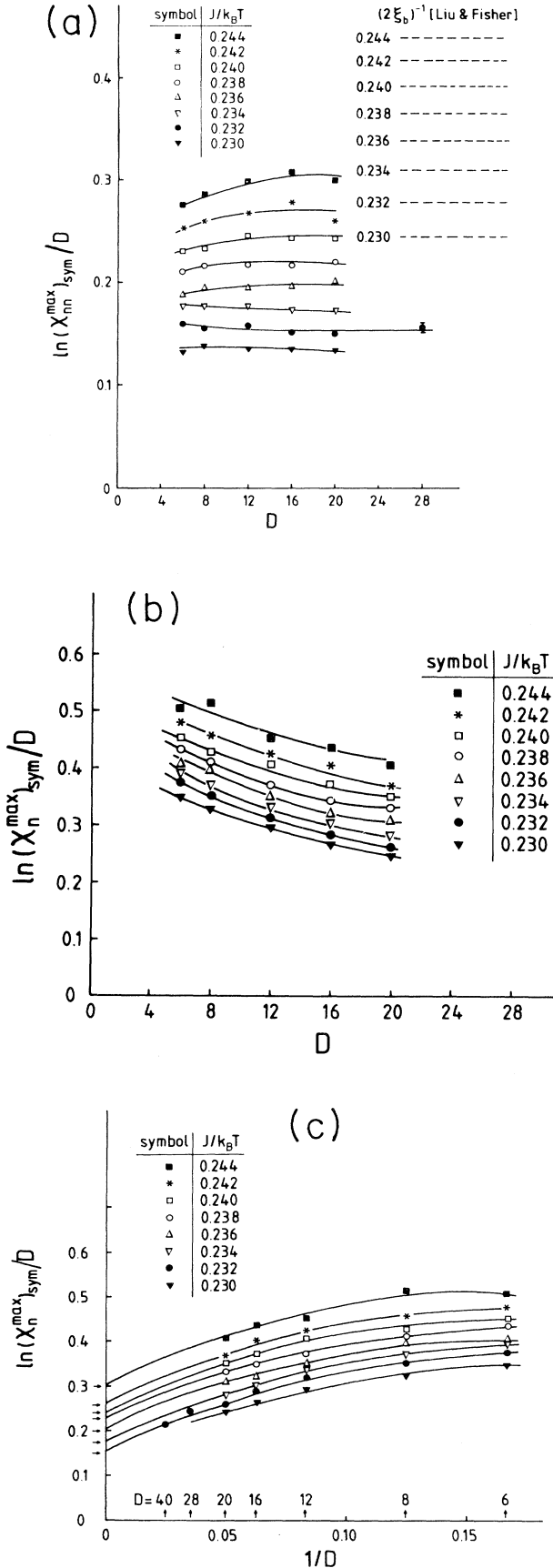
was taken from the analysis of low-temperature series expansions [40,42]. The disagreement between the actual value of l^{-1} and $(2\xi_b)^{-1}$ by nearly a factor of two at the highest temperature studied $(J/k_BT=0.23)$ decreases somewhat when the temperature is lowered (to about a factor of 1.5 at $J/k_BT=0.244$, where our estimate is least reliable).

We can offer only speculative explanations for the discrepancy between theory [9] and our simulation. This difference could be due to the fact that the interface in $d=3$ dimensions is not strictly localized as assumed by mean field theory, but, rather, delocalized (rough) due to capillary wave excitations. For a free interface in a semi-infinite system, these capillary waves would give rise to a mean-square fluctuation in the local interface position $\langle D^2 \rangle \propto l^2\ln(\tilde{L}/l)$ [43] on length scale $\tilde{L}$. In our confined geometry, one expects that the capillary wave spectrum exists only up to wavelengths of order $\xi_\parallel$, of course; using once again a mean field estimate [9] for $\xi_\parallel \propto \exp(D/4\xi_b)$ and equating $\tilde{L}$ with $\xi_\parallel$, we would obtain $\langle \Delta Z^2 \rangle \approx \xi_b D/4$ if we also identify the intrinsic length-scale l of the interface with ξ_b. In view of this simple argument, it is clearly tempting to define a characteristic width of the interface from the layer susceptibility profile itself:

$$\overline{Z_\chi^2} \equiv \sum_n \left[n - \frac{D+1}{2} \right]^2 \chi_{nn} / \sum_n \chi_{nn} . \tag{17}$$

However, as shown in Fig. 21, the data for $\overline{Z_\chi^2}$ are not consistent with a simple linear relation $\overline{Z_\chi^2} \propto D$ over the range of the thicknesses studied.

As is well known, if one considers a free interface whose spectrum is only limited by gravity, one must convolute the "intrinsic" interfacial profile with a Gaussian broadening due to capillary waves in order to obtain the total interfacial profile [43]. It would be of interest to develop a related theory for a fluctuating interface confined in a thin film. Such a treatment (which is beyond our scope here because we do not know the precise form of the capillary wave spectrum for wavelengths near $\xi_\parallel$) could possibly explain our data in Figs. 20 and 21. However, it is also conceivable that the intrinsic interfacial length l of Ising model interfaces is "renormalized" by fluctuations and differs from ξ_b by a constant factor of order unity. This question could be resolved by a high-precision study of Ising model interfaces in bulk (without confining walls), studying the above relation $\langle \Delta Z^2 \rangle \propto l^2\ln(\tilde{L}/l)$ as a function of an imposed length scale $\tilde{L}$ parallel to the interface. If such a renormalization of the intrinsic interfacial length scale l were to

FIG. 20. Plot of $\ln(J\chi_{nn}^{max})_{sym}/D$ vs D (a), $\ln(J\chi_n^{max})_{sym}/D$ vs D (b), and $\ln(J\chi_n^{max})_{sym}$ vs $1/D$ (c). Various temperatures are indicated by different symbols, and curves are guides to the eye only. The arrows on the ordinate scale (c) correspond to averages over the three largest thicknesses in (a). The broken horizontal straight lines in (a) are the predictions for $L^{-1}=(2\xi_b)^{-1}$ at the respective temperatures from the series expansion of Liu and Fisher [40].
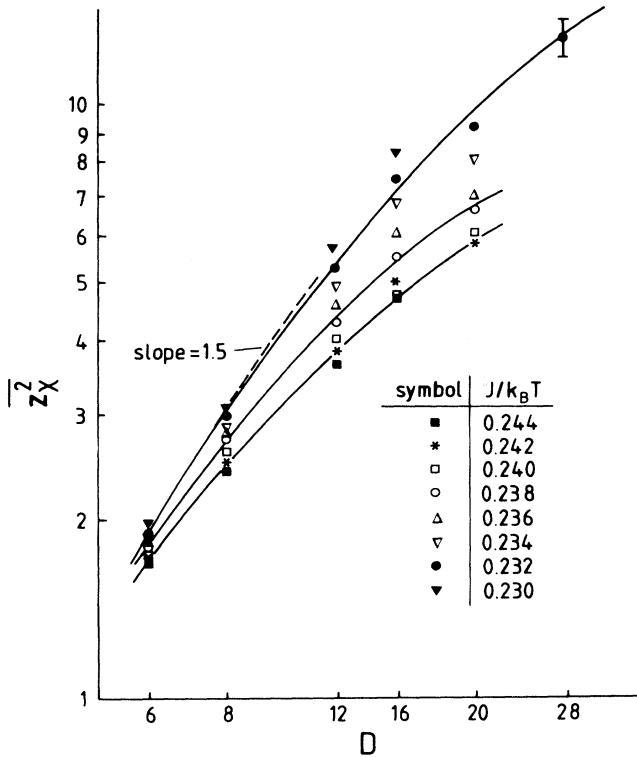
symbol	J/k_BT
■	0.244
*	0.242
□	0.240
○	0.238
△	0.236
▽	0.234
●	0.232
▼	0.230

FIG. 21. Log-log plot of $\bar{Z}_\chi^2$ vs D for various temperatures. Broken straight lines indicate that the initial increase is compatible with a behavior $\bar{Z}_\chi^2 \propto D^{1.5}$, but this clearly is not the asymptotic behavior.

occur, it would have a profound effect on the problem of critical wetting [15,26,44–52].

VI. CONCLUSIONS

In this paper, the first extensive Monte Carlo results have been presented for the phase transition [5–9] that occurs in systems with Ising-type symmetry confined in thin films between competing walls. We show that for large D and antisymmetric walls ($H_1 = -H_D$), a single phase transition occurs at a temperature $T_c(D)$ close to the wetting transition temperature $T_W(H_1)$ from a phase with a fluctuating interface centered in the middle of the film to a state where the interface is bound to either one of the walls. In agreement with the predictions of Parry and Evans [5,9], we find that this transition belongs to the universality class of the two-dimensional Ising model, but the observability of this Ising critical behavior is limited to a tiny region very close to $T_c(D)$ if D is large. For $T < T_C(D)$ the gradual unbinding of the interface from the wall at which it has been localized clearly can be interpreted as a wetting phenomenon. Since wetting in systems with short range forces is not fully understood

[15,26,44–52], the order of the wetting transition in this Ising film as well as the detailed character of the crossover between wetting and Ising behavior need to be elucidated. The Ising criticality is clearly observable only for rather small D.

An interesting aspect of these results is the gradual onset of the "high-temperature phase" (containing the fluctuating interface at $T_c(D) < T < T_{cb}$); the transition to that phase near T_{cb} is always rounded for all finite D, despite the fact that the system is infinite in the two remaining directions. Even in the limit $D \to \infty$, where a sharp specific heat singularity and divergent susceptibility appear at $T = T_{cb}$, there is no spontaneous magnetization present for $T_c(D \to \infty) < T < T_{cb}$, but only for $T < T_c(D \to \infty) = T_W(H_1)$. Of course, locally the system is then ordered, and one has stabilized two-phase coexistence with two equally large domains of opposite magnetization.

When exact antisymmetry ($H_1 \neq -H_D$) is lost, we argue qualitatively that this type of two-phase coexistence still exists but at a nonzero bulk field (Fig. 2). We suggest that the transition at $T_c(D)$ for $H_1 = -H_D$ is a special case of a line of critical points that contains the standard case of capillary condensation if $H_1 = +H_D$.

We confirm the prediction of Parry and Evans [9] that the phase at $T_c(D) < T < T_{cb}$ is characterized by susceptibilities varying exponentially with film thicknesses ($\ln\chi_n \propto D$, $\ln\chi_{nn} \propto D$), but we fail to find the prefactor (obtained from a mean field theory) in these relations. Tentatively, we attribute this discrepancy to the neglect of capillary-wave-type fluctuations in the mean field treatment, but again we cannot yet offer an alternative theory that would explain our findings quantitatively.

Thus, further work is clearly needed to produce a more complete picture of this transition. It also would be interesting to study cases where the corresponding wetting transition is clearly first order (e.g., Ising models where the exchange constant J_s in the layers adjacent to the walls exceeds the bulk exchange J sufficiently [26]). A qualitative characterization of Ising model interfaces between coexisting bulk phases is also called for. A further interesting extension of the models includes field gradients across the film [10]. We also hope that this study will stimulate the search for experimental realizations of such interfaces stabilized by boundary effects.

ACKNOWLEDGMENTS

[1] M. E. Fisher and P. G. de Gennes, Compt. Rend. Acad. Sci. (Paris) B **287**, 207 (1978).

[2] F. Brochard-Wyart and P. G. de Gennes, Compt. Rend. Acad. Sci. (Paris) B **297**, 223 (1983).

[3] E. V. Albano, K. Binder, D. W. Heermann, and W. Paul, Surf. Sci. **223**, 15 (1989).

[4] E. V. Albano, K. Binder, D. W. Heermann, and W. Paul, J. Stat. Phys. **61**, 161 (1990).

[5] A. O. Parry and R. Evans, Phys. Rev. Lett. **64**, 439 (1990).

[6] M. R. Swift, A. L. Owczarek, and J. O. Indekeu, Europhys. Lett. **14**, 475 (1991).

[7] J. O. Indekeu, A. L. Owczarek, and M. R. Swift, Phys. Rev. Lett. **66**, 2174 (1991).

[8] A. O. Parry and R. Evans, Phys. Rev. Lett. **66**, 2175 (1991).

[9] A. O. Parry and R. Evans, Physica A **181**, 250 (1992).

[10] J. Rogiers and J. O. Indekeu, Europhys. Lett. **24**, 21 (1993).

[11] For reviews, see M. N. Barber, in *Phase Transitions and Critical Phenomena,* edited by C. Domb and J. L. Lebowitz (Academic, New York, 1983), Vol. 8, Chap. 2.

[12] K. Binder, in *Phase Transitions and Critical Phenomena* (Ref. [11]), Vol. 8, Chap. 1.

[13] K. Binder, Thin Solid Films **20**, 367 (1974).

[14] K. Binder and D. P. Landau, J. Chem. Phys. **96**, 1444 (1992).

[15] For reviews of wetting phenomena, see S. Dietrich, in *Phase Transitions and Critical Phenomena* (Ref. [11]), Vol. 12, Chap. 1, and Ref. [16].

[16] D. E. Sullivan and M. M. Telo da Gamma, in *Fluid Interfacial Phenomena,* edited by C. A. Croxton (Wiley, New York, 1986), p. 45.

[17] P. G. de Gennes, Rev. Mod. Phys. **57**, 825 (1985).

[18] M. E. Fisher, J. Stat. Phys. **34**, 667 (1984); J. Chem. Soc. Faraday Trans. **282**, 1569 (1986).

[19] M. Schick, in *Liquids at Interfaces,* edited by J. Charvolin, J. F. Joanny, and J. Zinn-Justin (North-Holland, Amsterdam, 1990), p. 415.

[20] M. E. Fisher and H. Nakanishi, J. Chem. Phys. **75**, 5857 (1981).

[21] H. Nakanishi and M. E. Fisher, J. Chem. Phys. **78**, 3279 (1983).

[22] D. Nicolaides and R. Evans, Phys. Rev. B **39**, 9336 (1989).

[23] R. Evans, J. Phys. Condens. Matter **2**, 8989 (1990), and references therein.

[24] A preliminary account of some of our results was given in K. Binder, A. M. Ferrenberg, and D. P. Landau, in *Proceedings of the International Conference on Phase Transitions of Interfaces, Bad Herrenalb 1993* [Ber. Bunsenges. Phys. Chemie **98**, 340 (1994)] and in Ref. [25].

[25] K. Binder, D. P. Landau, and A. M. Ferrenberg, Phys. Rev. Lett. **74**, 298 (1995).

[26] K. Binder, D. P. Landau, and S. Wansleben, Phys. Rev. B **40**, 6971 (1989).

[27] Prior to Ref. [8], Eq. (6) was assumed in Ref. [3] in order to locate the wetting transition line $T_W(H_1/J)$ of the two-dimensional Ising model with a field H_1 at a one-dimensional surface.

[28] M. E. Fisher, in *Critical Phenomena,* edited by M. S. Green (Academic, London, 1971), p. 73.

[29] *Finite Size Scaling and the Numerical Simulation of Statistical Systems,* edited by V. Privman (World Scientific, Singapore, 1990).

[30] K. Binder, in *Computational Methods in Field Theory,* edited by C. B. Lang and H. Gausterer (Springer, Berlin, 1992), p. 59.

[31] Note that $k_B T_{cb}/J \approx 4.511\,42 \pm 0.000\,05$; see A. M. Ferrenberg and D. P. Landau, Phys. Rev. B **44**, 5081 (1991).

[32] E. Bürkner and D. Stauffer, Z. Phys. B **55**, 241 (1983); K. K. Mon, S. Wansleben, D. P. Landau, and K. Binder, Phys. Rev. B **39**, 70 89 (1989); K. K. Mon, D. P. Landau, and D. Stauffer, *ibid.* **42**, 545 (1990).

[33] M. Hasenbusch and S. Meyer, Phys. Rev. Lett. **66**, 530 (1991).

[34] P. C. Hohenberg and B. I. Halperin, Rev. Mod. Phys. **49**, 435 (1977).

[35] K. Binder and D. W. Heermann, *The Monte Carlo Method in Statistical Physics. An Introduction* (Springer, Berlin, 1988).

[36] K. Binder and D. P. Landau, J. Appl. Phys. **57**, 3306 (1985); Phys. Rev. B **37**, 1745 (1988).

[37] K. Binder and D. P. Landau, Phys. Rev. B **46**, 4844 (1992).

[38] K. Binder and D. P. Landau, Phys. Rev. Lett. **52**, 318 (1984); D. P. Landau and K. Binder, Phys. Rev. B **41**, 4768 (1990).

[39] T. W. Burkhardt and B. Derrida, Phys. Rev. B **32**, 7273 (1985); A. D. Bruce, J. Phys. A **18**, L873 (1985); D. P. Landau and D. Stauffer, J. Phys. (Paris) **50**, 509 (1989).

[40] A. J. Liu and M. E. Fisher, Physica **156A**, 35 (1989).

[41] M. Hasenbusch and K. Pinn, Physica **A192**, 342 (1993).

[42] We used the leading term of the power law quoted in Ref. [40], which agrees with the results of Ref. [41] within the statistical errors of the latter calculation. If we included the correction to scaling proposed in Ref. [40], the disagreement would even get worse. Analyzing the magnetization profile m_n at free surfaces choosing $H_1 = 0$ or slightly negative, we obtained ξ_b independently. These results again agree with the leading term of the Liu-Fisher analysis within statistical error.

[43] D. Jasnow, Rep. Prog. Phys. **47**, 1059 (1984).

[44] E. Brezin, B. I. Halperin, and S. Leibler, Phys. Rev. Lett. **50**, 1387 (1983).

[45] R. Lipowsky, D. M. Kroll, and R. K. P. Zia, Phys. Rev. B **27**, 4499 (1983).

[46] D. S. Fisher and D. A. Huse, Phys. Rev. B **32**, 247 (1985).

[47] K. Binder, D. P. Landau, and D. M. Kroll, Phys. Rev. Lett. **56**, 2276 (1986).

[48] R. Lipowsky and M. E. Fisher, Phys. Rev. B **36**, 2126 (1987).

[49] E. Brezin and T. Halpin-Healey, Phys. Rev. Lett. **58**, 1220 (1987); J. Phys. (Paris) **48**, 757 (1987).

[50] A. O. Parry and R. Evans, Phys. Rev. B **39**, 12 336 (1989).

[51] M. E. Fisher and H. Wen, Phys. Rev. Lett. **68**, 3654 (1992); K. Binder, D. P. Landau, and D. M. Kroll, Phys. Rev. Lett. **68**, 3655 (1992).

[52] A. J. Jin and M. E. Fisher, Phys. Rev. B **47**, 7365 (1993); M. E. Fisher, A. J. Jin, and A. O. Parry, Ber. Bunsenges. Phys. Chem. **98**, 357 (1994).